The Journal of Experimental Biology 203, 2623–2639 (2000)
Printed in Great Britain © The Company of Biologists Limited 2000
JEB2754

HYDRODYNAMICS, SHELL SHAPE, BEHAVIOR AND SURVIVORSHIP IN THE OWL LIMPET *LOTTIA GIGANTEA*

MARK W. DENNY* AND CAROL A. BLANCHETTE‡
Stanford University, Hopkins Marine Station, Pacific Grove, CA 93950, USA
*e-mail: mwdenny@leland.stanford.edu
‡Present address: Department of Ecology, Evolution and Marine Biology, University of California, Santa Barbara, CA 93106, USA

Accepted 6 June; published on WWW 9 August 2000

Summary

On wave-swept rocky shores, limpets are subjected to water velocities in excess of 20 m s^{-1}, which may impose large hydrodynamic forces. Despite the extreme severity of this flow environment, predictions from conical models suggest that limpets' shells are typically far from the optimal shape that would minimize the risk of dislodgment, a deviation that is allowed by the high tenacity of the limpets' adhesive system. In this study, we test this conclusion using an actual limpet. The shell of *Lottia gigantea* differs substantially from the hydrodynamic optimum in that its apex is displaced anteriorly to form a plough, which is used to defend the limpet's territory. The hydrodynamic effects of this shape are similar to those observed in conical models: the animal experiences an increased lift when facing into the flow and a decreased lift when the flow is at its back. However, neither effect has a substantial impact on the risk of dislodgment. When the animal is stationary, its adhesion to the substratum is very strong, and its risk of being dislodged is small regardless of its orientation to the flow and despite its sub-optimal shape. In contrast, when the animal is crawling rapidly, its adhesion is substantially decreased, and it would probably be dislodged by rapid flow even if the shell were shaped optimally. The risk of dislodgment by waves is therefore functionally independent of shell shape. In essence, despite the extremely high water velocities to which this species is subjected, its shell has had the 'permission' of the flow environment to respond to other selective factors, in particular those associated with its aggressive, territorial behavior. The result is a shell that is both a potent territorial weapon and a functional (albeit less than optimal) hydrodynamic shape.

Key words: limpet, hydrodynamic force, *Lottia gigantea*, shell morphology, evolution, lift, drag.

Introduction

Limpets (small marine gastropods with conical shells) are characteristic inhabitants of the intertidal zone of wave-swept rocky shores, and thus occupy one of the most physically stressful environments on earth. At low tide, intertidal animals are exposed to terrestrial conditions and the concomitant heat and desiccation stresses. At high tide as waves crash on the shore, water velocities greater than 10 m s^{-1} are common and impose large hydrodynamic forces. It is these hydrodynamic forces that are of particular interest here. For limpets, failure to resist these forces is tantamount to death. If dislodged from the substratum, they are likely to be washed onto the feeding tentacles of an anemone; even if they land on a benign patch of rock, they cannot easily right themselves if overturned.

Despite the large wave-induced forces placed on limpets and the dire consequences of dislodgment, measurements made by Denny (2000) suggest that the evolved shape of limpet shells has not been 'fine-tuned' to the flow environment. The lowest risk of dislodgment for a limpet is associated with a shell having a central apex and a height-to-length ratio of approximately 0.53. In fact, most limpets have an apex that is well anterior of the center of the shell, and a height-to-length ratio of approximately 0.34, only 63 % of the theoretical hydrodynamic optimum. Denny (2000) concludes that the exceptional ability of limpets to adhere to the substratum has pre-empted hydrodynamic forces from acting as a potent selective factor in the evolution of shell shape. In teleological terms, the evolution of a strong adhesive system has given limpets 'permission' to evolve shells whose shapes are hydrodynamically sub-optimal.

This conclusion was based on measurements conducted on model limpets – solid cones – and assumes a constant, high adhesive tenacity. There are at least three reasons to be skeptical of these results: (i) the shells of real limpets are not precisely conical; (ii) unlike the solid models, real limpets have semi-solid bodies that might affect the transmission of hydrostatic pressure to the underside of the shell, thereby affecting lift; and (iii) the adhesive tenacity of real limpets varies as a function of behavior and osmotic stress. Given these potential problems, can the conclusions of Denny (2000) be applied to real limpets?

In this study, we explore this question by examining one particular limpet species. *L. gigantea* (Sowerby) was chosen as our subject for two reasons. First, its shell is far from conical (it is typically rounded), and the apex is displaced far forward of the center of the shell. It is therefore an excellent example of deviation from the proposed optimal shape. Second, *L. gigantea* is an example of the potentially important interplay between hydrodynamics and behavior in the evolution of shell morphology. *L. gigantea* is aggressively territorial (Stimson, 1970); it uses its shell as a bulldozer to dislodge settling organisms and other intruders, thereby maintaining open space on the rock in which its algal food source can grow. The shell's shape reflects this behavior in that the anterior displacement of the apex forms a distinctive 'plough'. This shape functions admirably as an offensive weapon, but is very different from the predicted hydrodynamic optimum. As we will see, these real-world factors, which could potentially confound the theoretical approach of Denny (2000), in fact do not.

Lottia gigantea*: biogeography, morphology and ecology*

L. gigantea is found in the mid to upper intertidal zones of shores on the west coast of North America from Washington state to Baja California (Morris et al., 1980). The shell can reach a length of 9 cm, and a representative length of adults at our study site in central California is 5 cm. Fisher (1904) provides a thorough description of the anatomy of *L. gigantea*, and the aspects of morphology that have a bearing on the mechanics of adhesion are summarized in Fig. 1. The shell aperture is oval with its long axis running anterio-posteriorly. The muscular foot fills most of the aperture area and attaches to the substratum with a mucus adhesive. The foot is suspended from the shell *via* a horseshoe-shaped tendon that attaches to a distinct 'scar' on the shell's inner surface. Collagen fibers in the tendon fan out into the foot such that tension in the tendon and the attached muscles is broadly distributed to the foot's ventral adhesive area. The viscera lie between the foot and shell, with the head extending anteriorly through the open end of the foot's tendon. The viscera are enclosed by the mantle, a membranous structure that is anchored to the shell at the inner edge of the muscle scar. When the limpet is under water, pressure applied to the fluid around the animal can be transmitted to the viscera (and hence to the underside of the shell) either through the open space around the head or *via* the veins connecting the gills to the hemocoel. This transmission of pressure to the viscera is important when considering the lift imposed on the animal (see below).

L. gigantea typically inhabits vertical walls on wave-swept rocky shores, where it characteristically sits with its shell slightly elevated from the substratum (presumably to enhance water flow past the gills; Morris et al., 1980). When disturbed, however, the limpet clamps its shell tightly against the substratum, a response that substantially increases its adhesive tenacity. As with many intertidal invertebrates, *L. gigantea* has a dramatic escape response to contact with the predatory sea star *Pisaster ochraceus*. If the limpet's mantle is touched by a tubefoot from the sea star, the limpet lifts and rocks its shell and then rapidly crawls away. The speed of the animal during this response is much faster than when foraging. Although *L. gigantea* responds to starfish, at our site in central California it is typically found above the level at which *P. ochraceus* preys. Because of their large size and strong adhesive tenacity, adult *L. gigantea* appear to be immune to predation by birds and crabs.

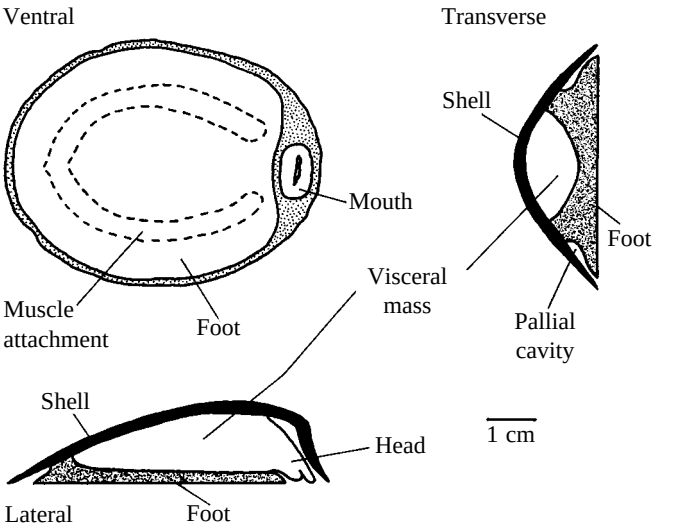

Fig. 1. The anatomy of *Lottia gigantea* Sowerby. For additional details, see Fisher (1904).

Abbott (1956) noted that on vertical walls *L. gigantea* are typically found with their heads pointing down, a behavior he proposed would aid in the flushing of wastes away from the animal. If wave-induced flow comes from below, this behavior might also serve to orient the animal head-on into the flow, a posture that (as we will see) is hydrodynamically disadvantageous.

Hydrodynamic forces

As water moves past a limpet, the pattern of flow is altered by the presence of the shell, resulting in a distribution of pressures around the shell that differs from that in the absence of flow. In steady flow, the pressure is typically high on the upstream face of the shell and within the body, and low on the dorsal and downstream aspects of the animal. The upstream–downstream and internal–external differences in pressure across the shell result in combined drag and lift forces tending to pull the limpet downstream and away from the substratum (see Denny, 1988, 2000; Vogel, 1994). Lift can be imposed on a limpet only if the hydrostatic pressures in the viscera and pallial cavity are different from the flow-induced pressures above the shell. But what is the pressure inside the shell during flow? Denny (2000) hypothesizes that in limpets the pressures in the viscera and pallial cavity are equal to the average pressure imposed at the ventral edge of the shell where it meets the substratum. This hypothesis implies that pressure is freely transmitted from the edge of the shell throughout the pallial cavity and viscera, and it is tested here.

If flow relative to the limpet changes through time or space,

a limpet shell may be exposed to an accelerational force, *I*. Unlike lift and drag, which are proportional to area (Denny, 1988, 2000; Vogel, 1994), the accelerational force is proportional to the volume, *V*, of fluid displaced by the limpet: $I=\rho VaC_M$. Here, ρ is the density of sea water (nominally 1025 kg m^{-3}; Denny, 1993), *a* is the acceleration of the fluid relative to the limpet, and C_M is the dimensionless inertia coefficient, an index of how the shape of the shell affects the accelerational force [see Batchelor (1967), Denny (1988) or Denny and Gaylord (1996) for a more complete discussion of the accelerational force].

Because the accelerational force scales with volume while velocity-induced forces (drag or lift) scale with area, the relative magnitudes of these forces vary with the size of the organism. For small organisms (such as the limpets dealt with here), the accelerational force is likely to be small relative to either lift or drag unless the acceleration is very large, the inertia coefficient is very large, or both (see Denny, 1988, 1989). Gaylord (1997, 1999) has measured the accelerations accompanying breaking waves and has recorded values in excess of 500 m s^{-2} at one of the sites used in the present study. But these rapid accelerations are applied over a very small spatial scale (less than 1 cm; Gaylord, 2000). As a result, the effective accelerations imposed on a limpet such as *L. gigantea* (with a length several times the scale of acceleration) are likely to be much smaller than the maxima measured by Gaylord (1997, 1999). For example, Gaylord (2000) simultaneously measured water velocity and the force imposed on a 5.3 cm diameter roughened sphere (C_M=2.2) and showed that the accelerational force was negligible compared with drag. Thus, unless the inertia coefficient of *L. gigantea* is large ($\geqslant$2.2), the imposed accelerational force is likely to be inconsequential. The C_M of *L. gigantea* is measured as part of the present study.

Materials and methods

We studied *Lottia gigantea* (Sowerby) at Hopkins Marine Station, Pacific Grove, California, USA, where they are a prominent and abundant member of the mid-to-high intertidal fauna on the most exposed areas of the shore.

Pressure measurements

We tested the ability of pressure to be transmitted from the external fluid to the pallial cavity and, hence, to the viscera and ventral surface of the shell. Two individuals were gently removed from the substratum and brought into the laboratory, where they were maintained in running sea water until used (less than 24 h). A small hole (1 mm diameter) was drilled in the center of the dorsal aspect of the shell, care being taken not to puncture the mantle. Using cyanoacrylate adhesive, a small piece of thick rubber sheet was glued over the hole to serve as a pressure seal, and a 20 gauge hypodermic needle was inserted through this seal into the space between the mantle and shell. The needle was connected by a 0.91 m length of seawater-filled flexible tubing to an arterial pressure transducer (Baxter Uniflow). The voltage output of the transducer (proportional to pressure beneath the shell) was amplified and recorded on a strip-chart recorder.

The limpet was placed on the floor of an aquarium, where it remained stationary. Sea water was then added to the aquarium to vary the hydrostatic pressure acting on the limpet. The depth of water in the aquarium (relative to the height of the needle's opening) was measured with a ruler. After a series of pressures had been applied to the limpet, the needle was removed from the animal and held in the aquarium at the level it had occupied in the shell. The water level was again varied and measured, providing a calibration for the pressure transducer.

Both limpets were alive and actively crawling on the day after testing.

Adhesive force

The ability of *L. gigantea* to adhere to the substratum was measured in the field. For each animal, the length, λ, width, *W*, and height, *H*, of the shell were measured with Vernier calipers. Length and width are used to estimate the aperture (planform) area, A_{pl}:

$$A_{pl} = \pi\lambda W/4 . \quad (1)$$

A loop of wire rope was then glued to the center of the shell's dorsal surface using epoxy putty, providing an attachment by which the limpet could be subjected to a simulated lift force. This force, which placed the foot and its adhesive in tension, was provided by the apparatus shown schematically in Fig. 2. The pointed rod at the base of the 'L'-shaped device provided a stable fulcrum about which the apparatus could rotate. When the experimenter pulled on the

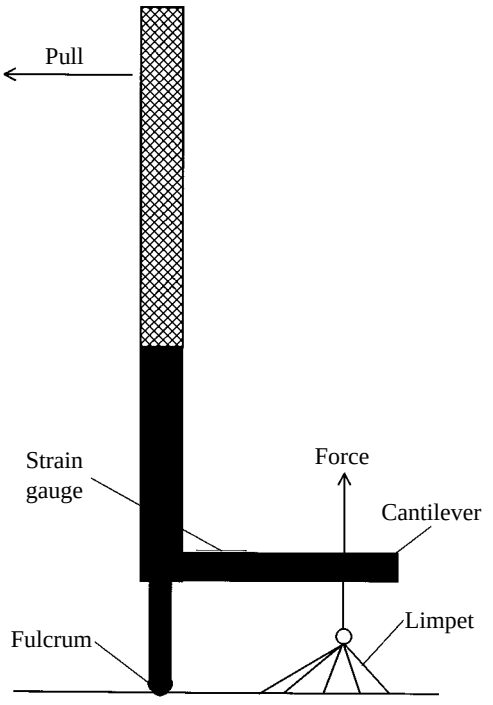

Fig. 2. A schematic diagram of the device used to measure the tensile adhesive tenacity of limpets.

handle, the end of the cantilever beam pulled dorsally on the limpet. The high stiffness of the limpet and apparatus ensured that the force vector remained perpendicular to the substratum throughout the experiment. The mechanical advantage of the apparatus allowed even large limpets to be dislodged, and the force of dislodgment was transduced by strain gauges attached to the base of the cantilever. The voltage output from the transducer (proportional to tensile force) was amplified and fed into an electronic peak detector, which recorded the maximum tensile force, F_T, that the organism could resist before being dislodged from the substratum. Eighty-one limpets were dislodged in tension. Their aperture areas ranged from 4.7 to 30.4 cm^2.

The ability of limpets to resist drag (a shearing force) was measured by looping a rope around the base of a pad of epoxy putty glued to the center of the shell and pulling on the loop parallel to the substratum. The level of the loop on the shell was approximately that of the shell's center of drag. The force, F_S, that the limpet could resist in shear was measured by a dual-beam strain-gauge transducer, the output of which was amplified and recorded as described above. Thirty limpets (with aperture areas ranging from 4.0 to 17.2 cm^2) were dislodged in shear. Lacking the mechanical advantage of the 'limpet wrench' of Fig. 2, this method was incapable of dislodging larger limpets.

For measurements in both tension and shear, the force was applied rapidly but not abruptly (over the course of 1–2 s).

For comparison with the tests described below, the osmotic status of each detached limpet was measured by taking a sample of fluid from the pallial cavity using a pipette. The osmolality of this fluid was measured using a Wescor 5000 vapor-pressure osmometer. At our site, C. Marzuola (unpublished data) measured the osmolality of both blood and fluid from the pallial cavity in the congeneric limpet *Lottia digitalis* and showed that the blood equilibrated with the fluid in the pallial cavity within approximately 2 h. In the light of this result, we use the osmolality of the pallial cavity fluid as an index of the blood osmolality in *L. gigantea*.

The forces of dislodgment for both tension and shear were measured at low tide when animals were stationary. For these measurements, the animal's shell was tapped several times prior to the application of force to give the limpet a chance to adhere as best it could. In addition, measurements of tensile strength were conducted under conditions designed to test the animal's adhesive capacity under adverse circumstances. In one series of tests, after the force transducer of Fig. 2 had been attached to the animal, the animal's mantle was touched with a *P. ochraceus* tube foot. A tensile force was then applied while the animal was in the midst of its escape response. Thirty-four limpets were dislodged while crawling in this manner; their aperture areas ranged from 6.6 to 32.5 cm^2. The defensive movements of the shell during the escape response precluded the measurement of shear strength while the animal was crawling, and it proved impossible to measure either tensile or shear strength during normal foraging locomotion. *L. gigantea* forages only when actively washed by waves (thus placing the experimenter at risk), and they stop crawling in response to even the slightest tug incidental to attaching a transducer.

A second series of tests was designed to measure the animal's response to the hyposaline conditions it might encounter when exposed to rain at low tide. A length of 'soaker' hose was attached to the rock wall above a population of limpets. Fresh water was sprayed onto the animals as the tide retreated, providing approximately 6 h of exposure to fresh water inundation. The tensile strength of limpets was then tested at low tide as described above. As an indication of the osmotic status of the limpets, a sample of the fluid in the pallial cavity was taken from each dislodged animal, and its osmolality was measured as described above. Forty-nine limpets were dislodged after being exposed to fresh water; their aperture areas ranged from 6.1 to 32.0 cm^2. For comparison, the osmolality of pallial-cavity fluid was measured for 10 limpets exposed at low tide to heavy natural rainfall.

Regardless of the type of force applied to the limpets, considerable variation was present in the force of dislodgment. Some of this variability is probably due to the variation in size of the limpets tested; larger limpets require more force to be removed from the substratum. To model this effect, ordinary least-squares regressions were fitted to the log-transformed data for shell aperture area and dislodgment force:

$$\ln F_P = \ln\alpha + \beta \ln A_{pl}, \quad (2)$$

where F_P is the force predicted for an animal of a given aperture and α and β are regression coefficients. The result for each experiment was an allometric equation of the form:

$$F_P = \alpha A_{pl}^{\beta}, \quad (3)$$

describing the trend between size and dislodgment force. (In this equation, α has been corrected for the bias introduced by the logarithmic transformation of the experimental data; Sprugel, 1983). Residuals from this best fit provide an estimate of the size-independent variability of adhesive force. Each measurement of dislodgment force was divided by the force predicted for an animal of that size (either in tension, $F_{P,T}$, or in shear, $F_{P,S}$) to give a dimensionless, normalized force, $F_{N,T}$ or $F_{N,S}$:

$$F_{N,T} = \frac{F_T}{F_{P,T}} \quad \text{or} \quad F_{N,S} = \frac{F_S}{F_{P,S}}. \quad (4)$$

The variability in these normalized forces can be described as a cumulative probability curve (Gaines and Denny, 1993). To construct this curve, the n normalized forces for a particular set of measurements are ranked, the smallest, $F_N(1)$, having rank i=1 and the largest, $F_N(n)$, having rank i=n. The probability (P) that a dislodgment force (measured for a limpet chosen at random) is less than $F_N(i)$ is estimated as (Gumbel, 1958):

$$P(i) = \frac{i}{n+1}. \quad (5)$$

Given the relatively small number of measurements in each

experiment (30–81), it is useful to fit an equation to these cumulative probability data as a means of estimating probability at values intermediate between those measured. A Weibull (lower bound) equation (Sarpkaya and Isaacson, 1981) was found to provide the most appropriate fit:

$$P(x) = 1 - \exp\left(-\frac{x-b}{c}\right)^{d}, \quad (6)$$

where b, c and d are constants chosen to minimize the squared error between the model curve and the empirical data. The regression was carried out using untransformed data and a simplex algorithm (Cacceci and Cacheris, 1984).

Direct measurement of the coefficients of lift, drag and inertia

As explained by Denny (2000), lift and drag were measured in a wind tunnel at Reynolds numbers, *Re*, equivalent to those found in the surf zone. Direct measurements of lift were conducted on three representative *L. gigantea* shells. Because the pressure distribution across the shell (which results in lift) can potentially be affected by the presence of the body beneath the shell, a model 'body' was constructed for each shell to mimic the presence of the foot. Each shell was sprayed with a mold release agent, and epoxy putty was molded to fill the inside of the shell. The shell was then clamped (aperture down) to a greased glass plate, thereby maintaining a smooth ventral surface to the 'foot' while the enclosed putty hardened. The molded 'body' was then removed from the shell and carved to remove putty from the pallial cavity, the area dorsal to the muscle scar (to simulate the cavity filled by the viscera) and adjacent to the head (to simulate the primary path by which pressure can be quickly transmitted to the viscera and thereby to the underside of the shell). The sculpted 'body' was then glued back inside the shell.

Lift, L, was measured using the nulling force transducer described by Denny (2000). The limpet was attached to the transducer with its apex in one of five orientations (0°, 45°, 90°, 135° or 180° to the oncoming wind), and a constant-velocity wind was imposed. After the lift had been measured, the velocity was changed, and lift was again ascertained. Mainstream wind velocities ranged from 6.5 to 51.3 $m\,s^{-1}$, corresponding to water velocities ranging from 0.6 to 4.6 $m\,s^{-1}$ (for sea water at 10 °C; see Denny, 2000).

Measurements of drag, D, for each of three limpet shells were conducted as described by Denny and Gaylord (1996) and Denny (2000). Drag was measured for three orientations, with the apex at 0°, 90° and 180° relative to the oncoming wind. For one shell, additional measurements were conducted with the apex at 45° and 135° from the oncoming wind. Measurements in the wind tunnel were supplemented by previous measurements made on a fourth shell in flowing water (Denny, 1995). These aquatic measurements were conducted in a flume (Denny, 1988) in a manner similar to those in the wind tunnel.

The projected areas of the experimental limpet shells were measured from photographs of the shells taken in different orientations. The planform area, A_{pl}, is the shell area projected onto the substratum when the shell is viewed from its dorsal side, and in this animal is virtually the same as the aperture area. Profile areas, A_{pr}, were obtained by photographing the shell's silhouette in a plane perpendicular to its aperture with the anterior of the shell at 0°, 45° or 90° to the camera. All areas were measured by projecting the appropriate photograph onto a sheet of paper and tracing around the shell. The scale of the photograph was determined from a ruler photographed along with the shell. The shell's silhouette and a known area were then cut from the paper and weighed, and A_{pl} or A_{pr} was calculated. Drag and lift coefficients were calculated according to equations 18 and 19 in Denny (2000).

The inertia coefficient, C_M, was measured for three shells using the technique of Denny and Gaylord (1996) and Gaylord (1997, 2000). In brief, each shell was attached to a flat plate held parallel to flow, and a transducer measured the force imposed on the limpet in the direction of relative flow as the plate was moved through a tank of stationary water. During an experiment, the plate was rapidly accelerated through the tank, and the resulting force (a combination of drag, the hydrodynamic accelerational force and the force required to accelerate the limpet's own mass) was recorded. Analysis of the time course of acceleration and correction for the limpet's mass allowed for the calculation of C_M. Measurements were conducted with the shell's anterior end at 0°, 90° and 180° to the oncoming flow.

Mapping shell topography

For use with the measurement of the pressure distribution over the shell, the shape of a representative shell was quantified. The shell was placed aperture-down on a horizontal surface, and an image of horizontal lines was projected horizontally onto the shell such that each line traced a path of equal altitude (an isocline). The shell was then photographed from above. Between photographs, the orientation of the shell was rotated about a vertical axis so that projected isoclines reached all aspects of the shell's dorsal surface. The vertical spacing between isoclines was measured by projecting the image on a wedge of known angle. The photographs of the limpet shell were magnified and traced onto paper to produce a topographical map of the shell, and this map was translated into digital form (Fig. 3) using mapping software (Surfer, version 5.0). Note that the anatomical apex of the shell (the site of the larval shell from which the adult shell grows, *AA* in the figure) is anterior to the 'topographical' apex (*TA*, the highest point on the shell).

The pressure distribution over shells

The pressure distribution acting on the dorsal surface of a *L. gigantea* shell was measured using the technique described by Denny (2000). In brief, an epoxy cast was made of the representative *L. gigantea* shell, and 49 pressure ports 0.6 mm in diameter were drilled through its dorsal surface (see Fig. 3). The shell was attached to the wall of the wind tunnel, and wind of a known velocity was imposed. The pressure at each port

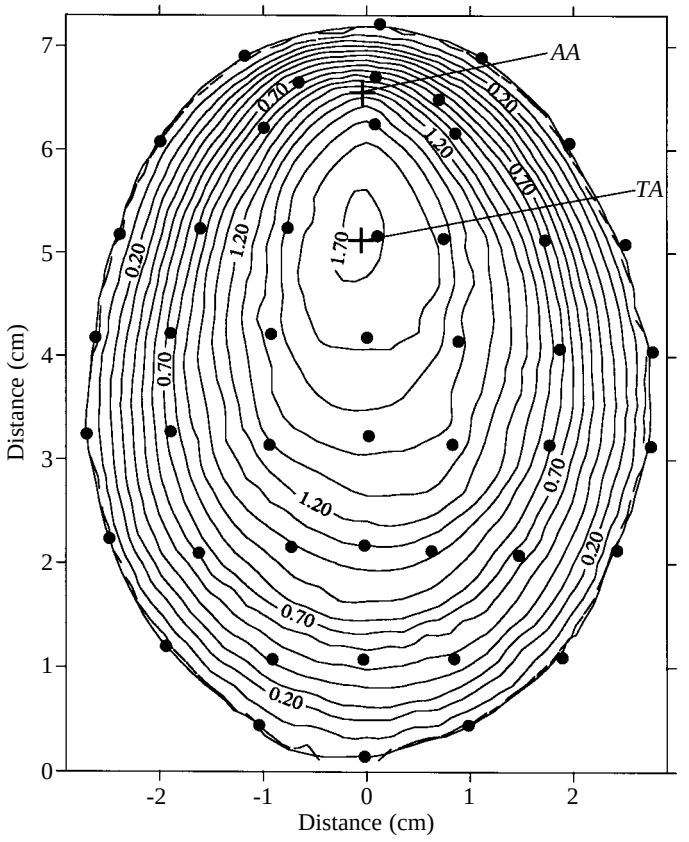

Fig. 3. A topographical map of the representative *Lottia gigantea* shell used to measure the pressure distribution. Note that the topographical apex, *TA*, is substantially aft of the anatomical apex, *AA*. Filled circles mark the locations of pressure ports.

on the shell (as well as the dynamic pressure of the wind) was measured using a bank of alcohol manometers. From these measurements, mapping software (Surfer) was used to estimate the distribution of pressures acting at each node of an orthogonal grid projected onto the planform area of the shell. The measurements of the shell's topography (Fig. 3) allowed for an estimation of the local tilt of the shell at each of these nodes. From the combined information regarding the local pressure and tilt of the shell, it was possible to calculate the pressure drag imposed on the shell as well as the pressure-induced force applied to the shell's dorsal surface. The pressure acting on the fluid in the pallial cavity (and, hence, on the underside of the shell) was estimated as the average of the pressures recorded at the shell's periphery. The net lift, *L*, acting on the limpet could therefore be calculated from the difference in pressure between the dorsal and ventral surfaces of the shell. In addition, the measured distribution of pressures allowed for the calculation of the center of drag and the center of lift. See Denny (2000) for details of these calculations.

Pressure distributions were measured for wind velocities varying from 13.5 to 51.3 $m\,s^{-1}$, corresponding to water velocities (sea water, 10 °C) of 1.2–4.6 $m\,s^{-1}$. The model shell was oriented with its anterior end at 0 °, 45 °, 90 °, 135 ° and 180 ° to the oncoming wind.

Maximum water velocity

The maximum wave-induced water velocities imposed on the areas inhabited by *L. gigantea* were estimated using a modification of the recording dynamometer developed by Bell and Denny (1994). A stainless-steel spring is attached to a drag element (a wiffle golf ball) *via* a short length of braided nylon fishing line. Drag imposed on the ball extends the spring, and the maximum extension is recorded by a slider threaded onto the string. The housing for the spring (a section of 12 mm diameter chlorinated polyvinyl chloride tubing) is mounted in a hole drilled into the substratum such that the ball is the only part of the apparatus protruding from the rock. A slot milled into the side of the tube provides access to the slider. To carry out a measurement, the slider is reset, the apparatus is inserted into the rock, and the dynamometer is left to respond to the flow for one to several days. After retrieval, the displacement of the slider (proportional to maximum force) is measured using Vernier calipers. The stiffness of the spring is calibrated by mounting the dynamometer vertically (ball down) and hanging known weights from the ball. In total, 33 dynamometers were installed on four vertical rock faces inhabited by *L. gigantea*, and forces were recorded at intervals of 3–7 days for 20 months.

The drag coefficient of wiffle golf balls has been measured by Bell and Denny (1994), allowing the maximum forces recorded in these experiments to be translated into a corresponding maximum water velocity (using the standard model for drag; see equation 3 of Denny, 2000). Given that the drag coefficient of the balls was measured in steady flow, whereas the flows imposed by waves can change abruptly, there is some question as to the accuracy of this translation from drag to velocity. For example, Gaylord (2000) simultaneously measured water velocity and the force on a rigidly mounted ball in the surf zone and found that, as a wave impinged on the ball, the force was on average 1.89 times the force that would be predicted from the standard model of drag (equation 3; Denny, 2000). It is currently unclear whether a similar factor would apply to the flexibly mounted ball on the dynamometer. In the light of this possible effect, we refer to the maximum velocities estimated from dynamometer recordings as 'equivalent velocities'. Actual velocities are likely to be less than or equal to these equivalent velocities.

Orientation of limpets in the field

The orientation of limpets was measured to test the assertion (Abbott, 1956) that *L. gigantea* orient with their head down on vertical walls. Three walls were chosen at Hopkins Marine Station, and the orientation of the anterior–posterior axis of each limpet was measured to the nearest degree using an electronic level (SmartLevel, Wedge, Inc.). In these measurements, 0 ° corresponds to a horizontal shell axis with the apex to the right, 90 ° to the apex straight up and 270 ° to the apex straight down. In total, 172 *L. gigantea* were measured. Circular statistics (Zar, 1974) were used to determine whether the orientation of limpets was non-random.

Survivorship

The survivorship of *L. gigantea* was measured on a fully exposed, vertical wall at Hopkins Marine Station. This wall is isolated by surge channels from nearby *L. gigantea* habitats, inhibiting immigration and emigration. In December 1997, every limpet of taggable size (length greater than approximately 28 mm, a total of 65) was marked with a small, numbered tag glued to its shell, and the length of the shell was measured using Vernier calipers. The survival of this population was subsequently assessed in June 1998.

Theory

Forces

To estimate the survivorship of *L. gigantea* on wave-swept shores, we relate the hydrodynamic forces imposed by breaking waves to the ability of the limpet to resist these forces using the mechanics described by Denny (2000). In short, the limpet's shell sits with its margins in contact with the substratum, held in place by the adhesive attachment of the foot. The foot is modeled as an elliptical disk with the same area as the aperture of the shell (A_{pl}). In an actual limpet, the foot is suspended from the shell by a muscular tendon (Fig. 1); thus, any force applied to the shell is distributed along this tendon. The pattern of force distribution is difficult to estimate on purely anatomical grounds, however, because the tension at any point in the tendon is a result not only of the force applied to the shell but also of the active tension in the muscles of the foot. As a practical alternative to a precise model of distributed force, a simplified model is used here. All force applied to the shell is assumed to be transmitted to the foot through a linkage located in the center of the aperture, and the foot is assumed to be a rigid, adhesive disk (see Fig. 7 in Denny, 2000).

Drag has two effects on the shell/foot mechanism. First, it tends to push the shell downstream, applying a shearing force to the foot. Second, because drag acts above the plane of the aperture (at the center of drag), there is a tendency for drag to cause the shell to rotate about a horizontal axis. The upstream edge of the shell will tend to be lifted and the shell will tend to rotate about its downstream edge. In a similar fashion, lift has two effects on the shell. First, there is a tendency to pull the shell away from the substratum. Second, lift has a tendency to cause the shell to rotate. As we will see below, the center of lift is generally downstream of the center of the shell and, as a result, lift tends to raise the downstream edge of the shell. The net torque acting on the shell is the sum of the torques applied by drag and lift. If the shell is to be in rotational equilibrium, any net moment must be resisted by a countermoment supplied by a tensile force acting on the foot.

Stresses

The shear stress τ (shear force per area) applied to the adhesive beneath the foot is:

$$\tau = \frac{D}{A_{pl}} = \frac{C_D A_{pr} p_d}{A_{pl}} , \quad (7)$$

where D is drag, C_D is the drag coefficient, and p_d is the dynamic pressure:

$$p_d = \tfrac{1}{2}\rho u^2 . \quad (8)$$

Here, u is the water velocity relative to the animal. Because drag varies with water velocity, shear stress is a function of the flow environment. A flow-independent index of shear stress, τ', can be obtained, however, by dividing τ by the dynamic pressure:

$$\tau' = \frac{\tau}{p_d} = \frac{C_D A_{pr}}{A_{pl}} . \quad (9)$$

In a similar fashion, the tensile stress σ acting on the adhesive beneath the foot (due both to the direct action of lift and to the combined moments of lift and drag) is:

$$\sigma = \frac{T}{A_{pl}} , \quad (10)$$

where T is the tensile force. σ can be normalized to the dynamic pressure:

$$\sigma' = \frac{\sigma}{p_d} . \quad (11)$$

These values for dimensionless stress can be compared directly with those measured by Denny (2000) for conical models of limpets.

Results

Shell morphology

The ratio of length to width is very nearly constant among individuals (W=–3.120+0.811λ, both in mm, r^2=0.964, P<0.001, N=167), while the ratios of height to length and height to width are more variable (H=0.125+0.224λ, r^2=0.717, P<0.001; H=1.358+0.265W, r^2=0.688, P<0.001; N=167 in both cases).

Internal pressure

The pressure beneath the shell varied through time, typically rising rapidly when the animal moved its shell, and then gradually decreasing to a basal level when the animal was quiescent. These basal pressures closely paralleled the hydrostatic pressure applied to the limpet (Fig. 4): pressure under the shell equals 112 Pa + 1.006 times the static pressure in the water surrounding the limpet (r^2=0.989, P<0.001, N=41). The slight, constant offset between basal pressure and ambient hydrostatic pressure may be due to the inadvertent injection of a small amount of sea water into the space between the mantle and shell during the attachment of the pressure transducer or to the internal pressure maintained by muscular contraction in the limpet. The similar variation between basal and hydrostatic pressures suggests that the static pressure present in the pallial cavity can readily be transmitted to the underside of the shell, as assumed by Denny (2000).

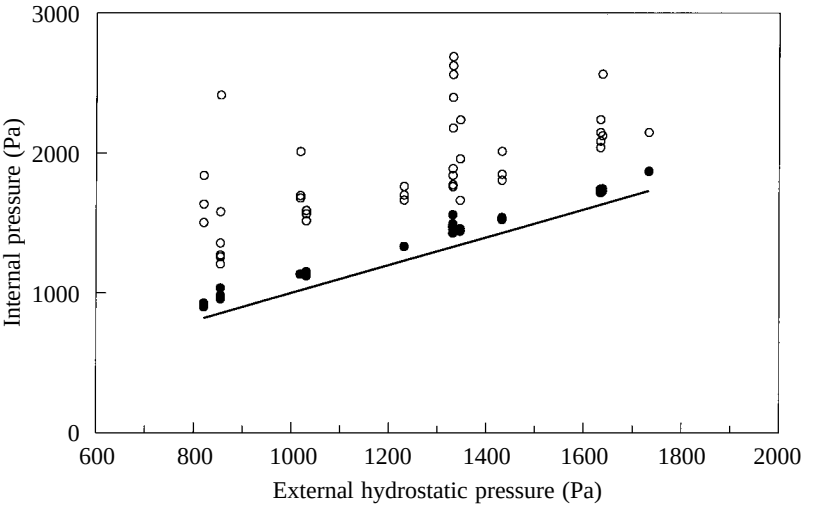

Fig. 4. The variation in measured internal pressure beneath a limpet shell as a function of the applied external hydrostatic pressure. Filled circles are measurements taken when the shell had been still for a time sufficient to allow the internal pressure to return to a basal value; open circles denote peak pressures during movement of the shell. The line denotes equivalence between internal and external pressure.

Adhesive forces

Allometric equations describing the variation in dislodgment force as a function of limpet size are plotted in Fig. 5, and the coefficients are given in Table 1. The adhesive tenacity of stationary *L. gigantea* is very high. For example, a limpet 5 cm in length requires the application of 190 N to be dislodged in tension and 382 N in shear.

A larger tensile force is required to dislodge a limpet when it is stationary than when it is moving rapidly. For example, a 5 cm long limpet will be dislodged by a tensile force of only 38 N when crawling as opposed to 190 N when stationary.

On average, limpets subjected to hypo-osmotic stress (the osmolality of pallial fluid is 738±12 mosmol kg^{-1}, mean ± S.E.M., N=10) required more force to dislodge than limpets of normal osmolality (1056±5 mosmol kg^{-1}, mean ± S.E.M., N=84). For comparison, the osmolality of sea water was

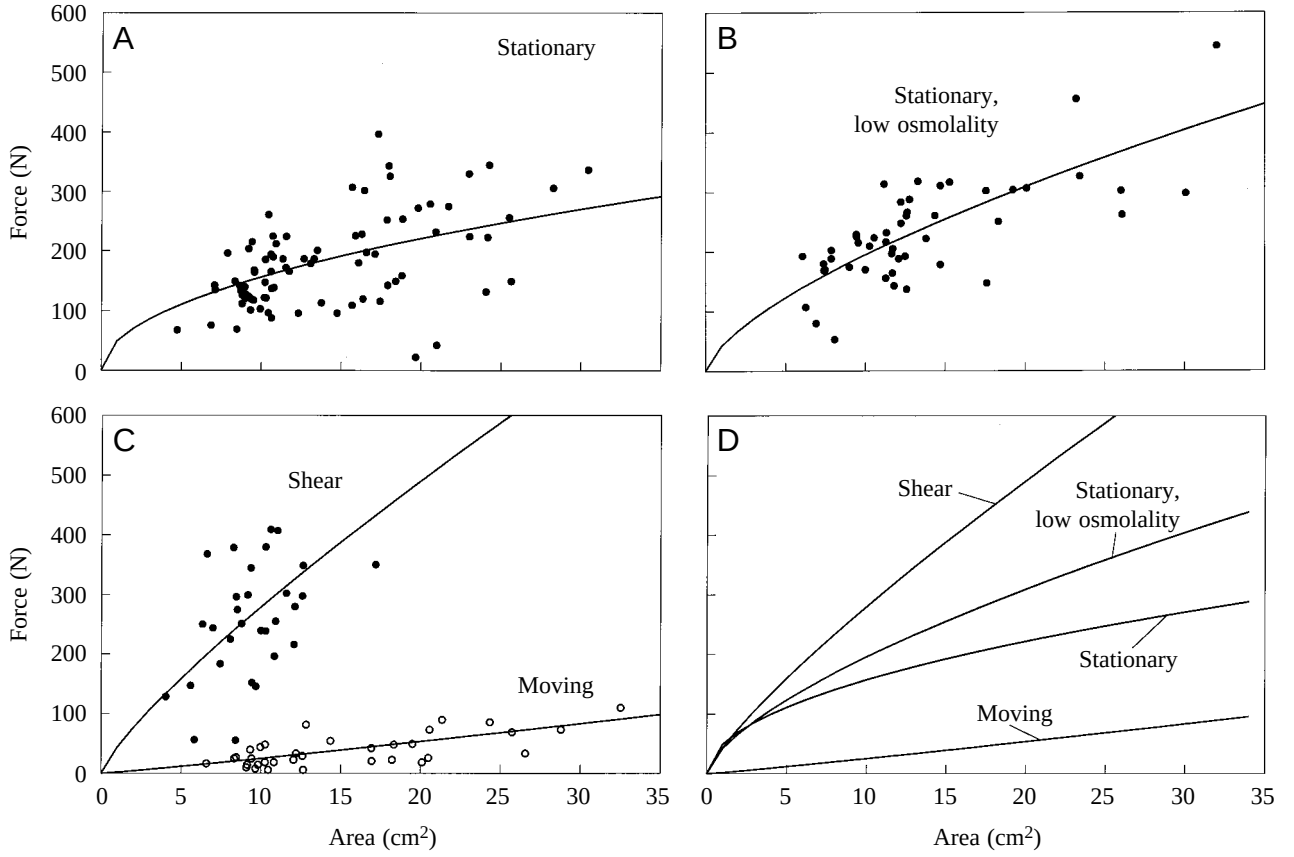

Fig. 5. Predicted (lines) and measured (circles) dislodgment force as a function of aperture area. Table 1 provides the equations from which these regression curves are drawn.

Table 1. *Regression coefficients for dislodgment force as a function of planform area (see equation 3)*

	α	β	*N*	r^2	*P*
Tension					
Stationary (dry)	4884	0.498	81	0.162	<0.001
Stationary (rain, =low osmolality)	19120	0.664	49	0.444	<0.001
Crawling	50471	1.103	34	0.360	<0.001
Shear	76301	0.812	30	0.224	<0.01

Table 2. *Coefficients for the cumulative probability curves of residual force (see equation 6)*

	b	*c*	*d*	r^2	*P*
Tension					
Stationary (dry)	-6.111×10^{-4}	1.089	3.281	0.996	<0.001
Stationary (rain, =low osmolality)	−3.760	4.865	21.390	0.997	<0.001
Crawling	-4.960×10^{-4}	1.0982	1.8435	0.991	<0.001
Shear	-5.036×10^{-4}	1.092	3.184	0.981	<0.001

987 mosmol kg^{-1}, and limpets sampled on a rainy day had pallial fluid with an osmolality of 929±26 mosmol kg^{-1} (*N*=10). There is considerable variation within these allometric models for dislodgment force (see the low r^2 values in Table 1, which quantify the fraction of the overall variance that is accounted for by the regression model for the size of the animal).

The cumulative probability curves of the normalized residuals from the regression models of force are shown in Fig. 6. In each case, the curves closely match the data (r^2>0.98 for the predicted value *versus* the actual value, Table 2).

Drag and lift coefficients

Drag coefficients as a function of Reynolds number are shown in Fig. 7 together with the regression curves that model the data. In general, there is little variation in C_D with *Re*, and (with the exception of limpets oriented broadside to the flow, Fig. 7C) there is little variation among individuals. The highest drag coefficients occur when the limpet's anterior end is 90° or 135° to the oncoming flow. With the exception of limpets broadside to the flow, drag coefficients measured in water (filled circles) are similar to those measured in air (open circles). The reason for the variation in broadside C_D among individuals is not apparent. We assume that drag at this orientation is simply more sensitive to slight variations in shell shape than is drag when the axis of the shell is parallel to the flow.

Lift coefficients calculated from direct measurements are

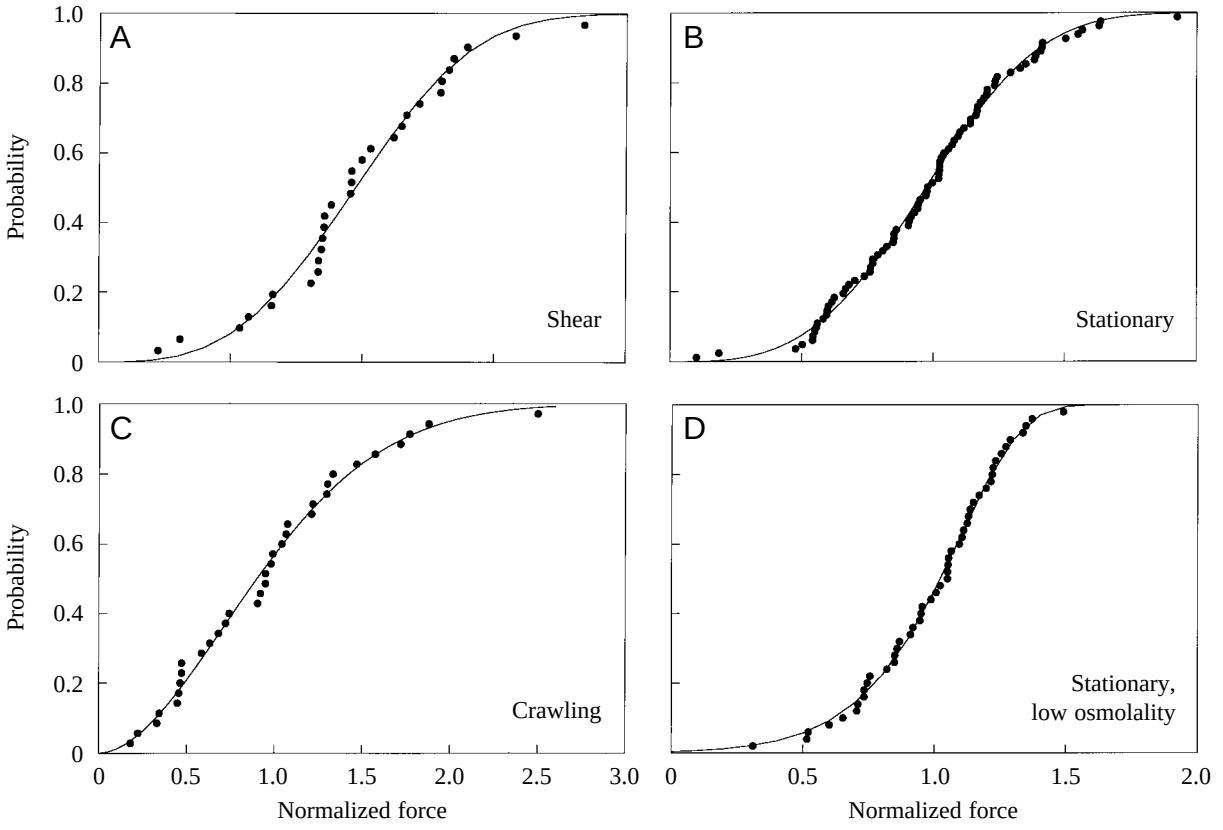

Fig. 6. Cumulative probability of dislodgment as a function of normalized force. The regression equations from which the solid curves have been drawn are given in Table 2.

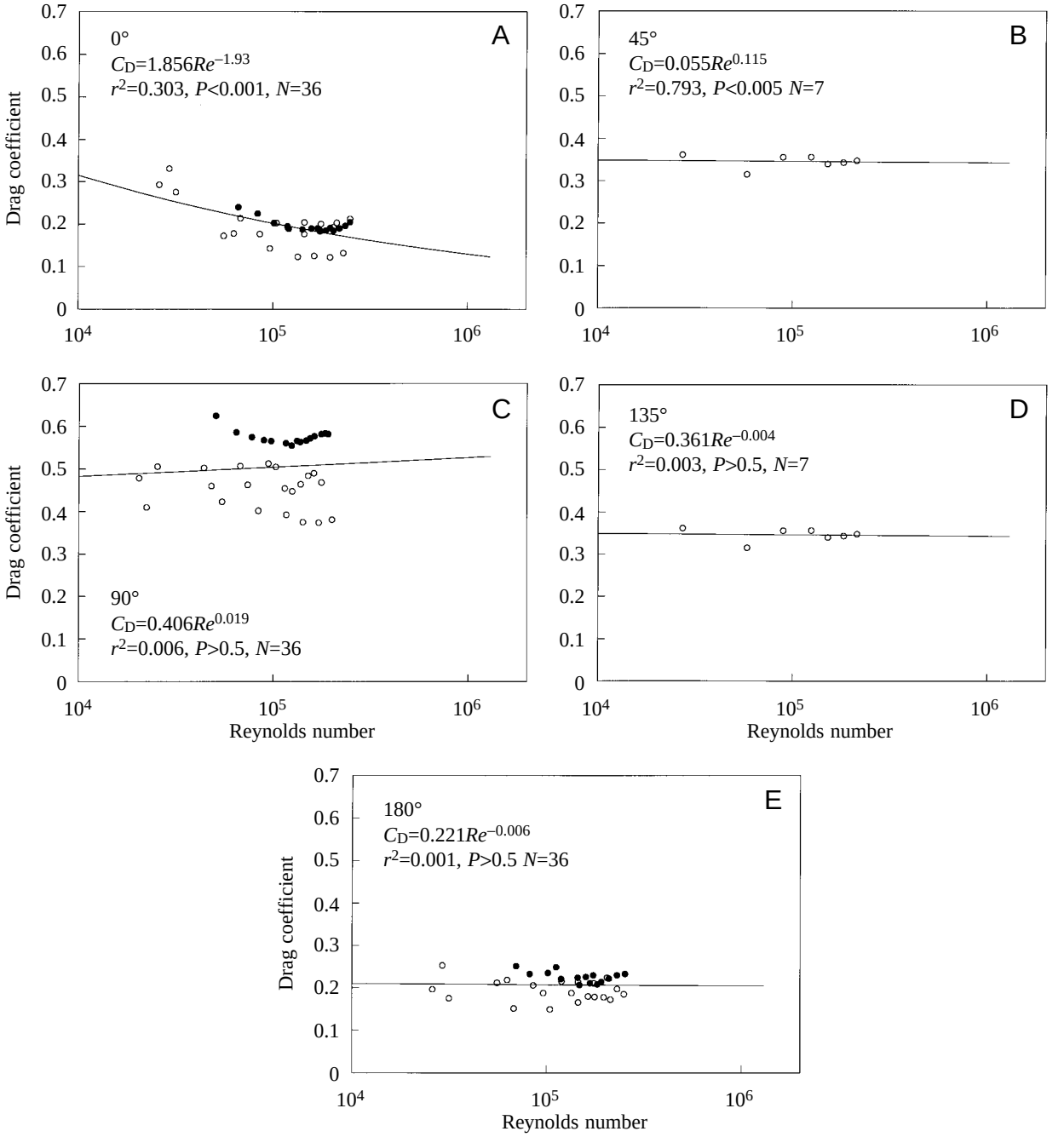

Fig. 7. Drag coefficient, C_D, as a function of Reynolds number, *Re*, and shell orientation relative to the flow. The filled circles denote measurements made in water; the open circles are for measurements made in air. The solid curves are regressions fitted to the data.

shown as a function of Reynolds number in Fig. 8 (filled circles) together with the regression curves that model the data. In general, C_L decreases slightly at higher Reynolds numbers and, except for a noticeably lower lift coefficient when the posterior edge of the shell is upstream (Fig. 8E), there is little variation in C_L with orientation relative to the flow.

Two sets of lift coefficients were calculated from pressure distributions and are also shown in Fig. 8. In one case, the pressure acting on the ventral side of the shell was assumed to be the average pressure measured around the shell's periphery. These estimates (open circles in Fig. 8) are slightly lower than the lift coefficients measured directly, suggesting that the pressure under the shell is slightly higher than the average pressure acting at the periphery of the shell. In contrast, lift coefficients calculated on the assumption that the pressure beneath the shell is equal to the (relatively high) local static pressure (open triangles in Fig. 8) are slightly larger than the lift coefficients based on direct measurements. Evidently, although the pressure underneath the shell is not as low as the average peripheral pressure, it is lower than the hydrostatic

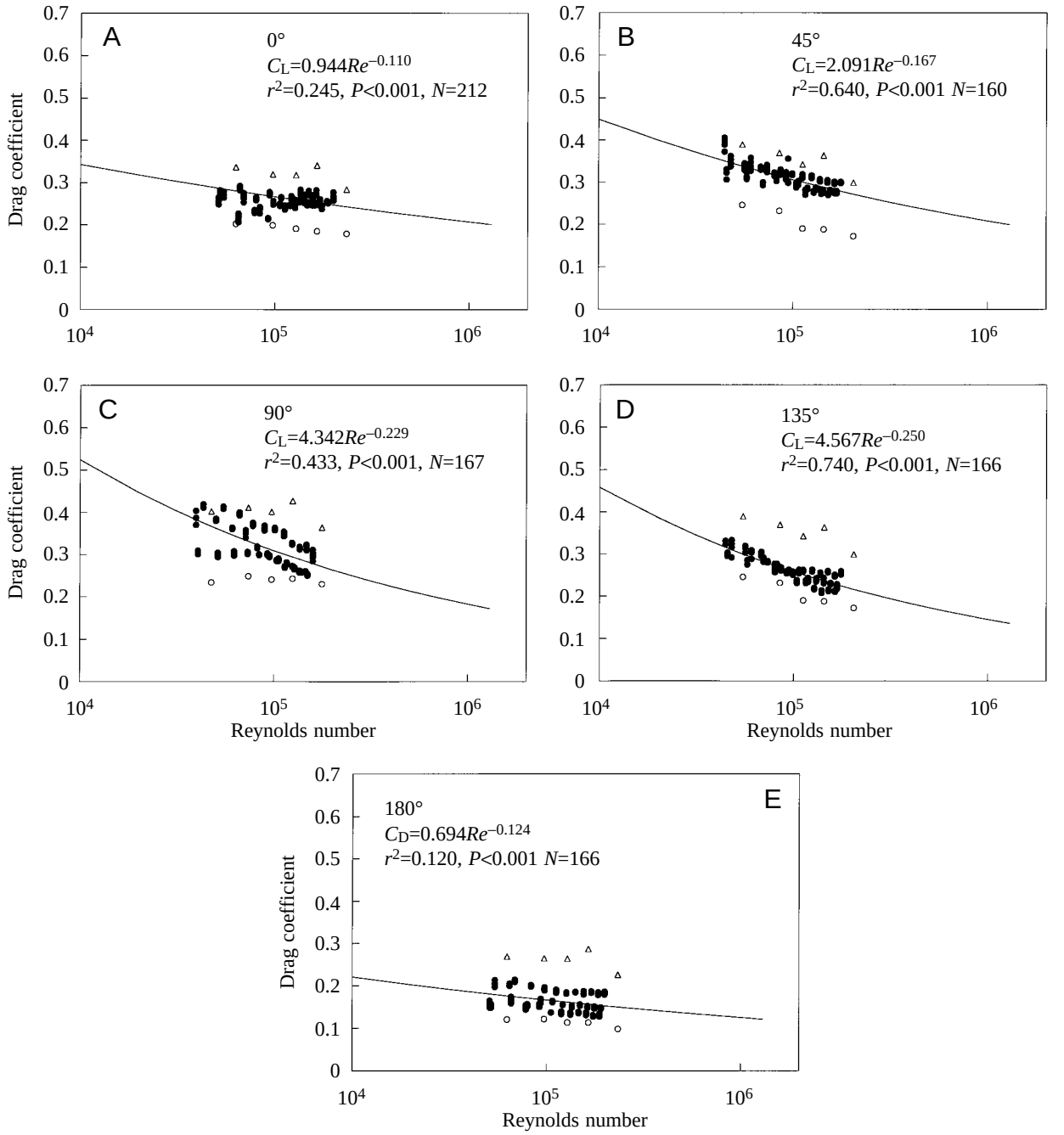

Fig. 8. Lift coefficient, C_L, as a function of Reynolds number, *Re*, and shell orientation. The filled circles denote direct measurements. The open circles denote estimates made on the assumption that the pressure beneath the shell is equal to the average pressure at the shell's periphery. The open triangles denote estimates made on the assumption that the pressure beneath the shell is equal to static pressure. The solid curves are regressions fitted to the filled circles.

pressure, an indication that the sub-shell pressure is indeed affected by the flow.

Both the drag and lift coefficients measured here closely match those predicted by Denny (2000) for cones of a similar height-to-length ratio.

Coefficient of inertia

The coefficient of inertia is 1.36±0.07 when the limpet is oriented with its anterior upstream, 1.30±0.07 with the shell broadside to flow and 1.44±0.15 with the posterior of the shell upstream (means ± S.D., N=3 in all cases). These values are similar to that of a smooth sphere (C_M=1.5) and are less than that of the roughened sphere used by Gaylord (1997, 2000) in his field experiments (C_M=2.2). Gaylord (1999, 2000) found that, with this magnitude of inertia coefficient, the accelerational force made a negligible contribution to the

Table 3. *The moment arms associated with lift and drag*

Angle (degrees)	Lift lever arm, y_{lc}	Drag lever arm, z_{dc}
0	+0.04	0.30
45	+0.02	0.28
90	–0.04	0.15
135	–0.09	0.06
180	–0.13	0.20

Values given for lift are the ratio of lever-arm length to the length of the shell in the direction of flow. Positive values denote moments that act in the same direction as the moment due to drag; negative values denote moments that act in opposition to the moment due to drag.

The values given for drag are the ratios of the lever-arm length to the height of the shell.

overall force on a sphere with a diameter similar to that of large *L. gigantea*. We conclude, therefore, that the accelerational force is not likely to form a substantial fraction of the overall force imposed on the limpet.

Pressure distributions

The pressure distributions over *L. gigantea* shells are similar to those reported by Denny (2000) for cones (see his Figs 16B,D, 17B). Pressure is highest at the lowest elevations of the upstream face of the shell and is lowest at high elevations lateral to and downstream of the shell's topographical apex. The center of pressure never strays far from the vicinity of the center of the shell; the maximum offset occurs when the shell's posterior end is upstream. The lever arms associated with the center of drag and pressure (z_{dc} and y_{lc}, respectively) are given in Table 3. When the anterior end of the shell is directly upstream or at 45 ° to the flow, the center of pressure is slightly upstream of the center of the aperture. In all other orientations, the center of pressure is downstream of the center of the aperture.

Maximum water velocity

Twenty months of measurements confirmed the assumption that water velocities are exceptionally high in the surf zone. Equivalent water velocities of 10–15 m s^{-1} were common on the four vertical walls inhabited by *L. gigantea*, and extreme values were 18, 19, 19 and 24 m s^{-1}.

Flow-induced shear and tensile stress

The tensile stress placed on the foot is larger than the shear stress at all shell orientations (Fig. 9). Recall that the adhesive tenacity in tension is substantially less than that in shear (Fig. 5). Thus, *L. gigantea* experiences the greatest stress in the direction in which its adhesion is weakest, and it seems likely that tension rather than shear will dislodge the organism. In the light of this fact, we concentrate on the consequences of tensile stress.

The orientation-dependent variation in non-dimensional tensile stress is shown in Fig. 10. In this figure, stress is displayed in a polar plot as a function of the orientation of the limpet to the flow. Here, the flow comes from the top of the page at an angle defined to be 0 °. If a line is extended from the origin in the direction of the shell's anterior–posterior axis, the length of that line when it crosses the curve of dimensionless stress is proportional to the dimensionless stress on the shell at that particular orientation. For example, if the limpet's apex is at 90 ° to the oncoming flow, the dimensionless stress at a velocity of 25 m s^{-1} is approximately 0.20. The limpet experiences the greatest tensile stress when its anterior end is at 45 ° to the flow, and tensile stress is minimal when the posterior end of the shell is upstream. At the highest water velocity likely to occur at our site (25 m s^{-1}) and for angles between 0 ° and 90 °, dimensionless stress for *L. gigantea* is greater than that for a right (symmetrical) cone of the same ratio of height to length (shown by the broken line in Fig. 10). At the same high water velocity and for angles between 90 ° and 180 °, dimensionless stress on the limpet is less than that for a symmetrical cone of the same ratio of height to length. Dimensionless stress decreases with increasing water velocity at all angles relative to the oncoming flow, an effect due primarily to the decrease in lift coefficient with increasing Reynolds number (Fig. 8).

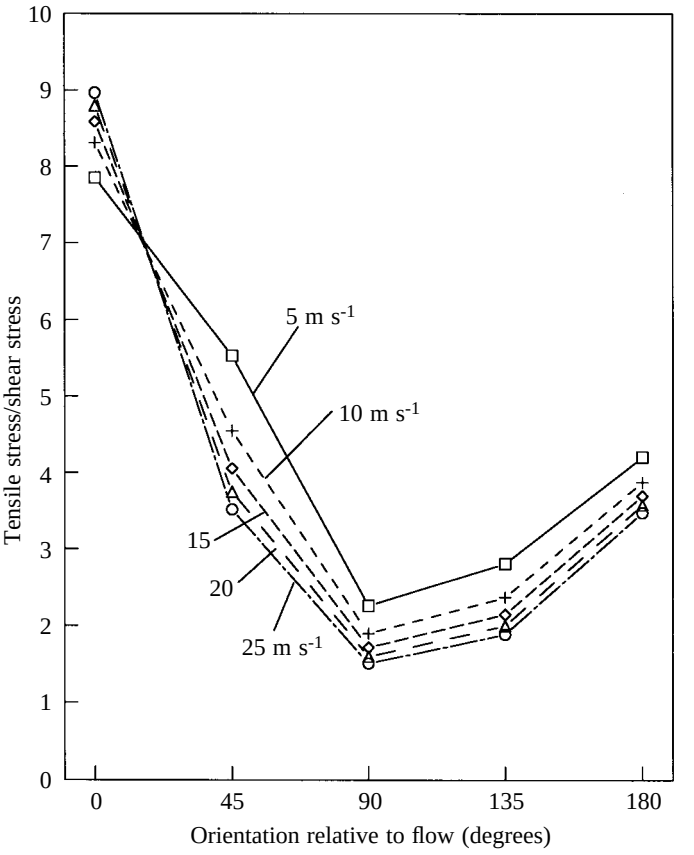

Fig. 9. The ratio of tensile stress to shear stress as a function of shell orientation and water velocity. Tensile stress is always higher than shear stress.

Risk of dislodgment

The data presented above can be used to estimate the

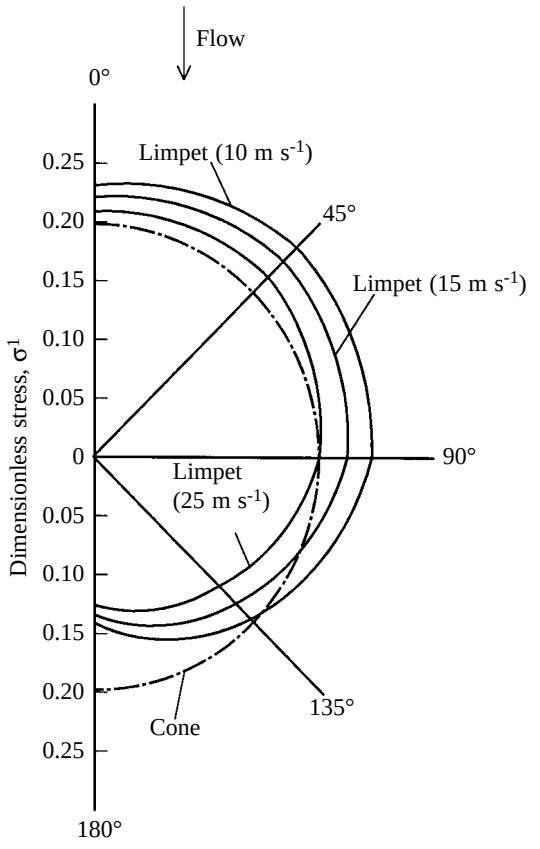

Fig. 10. Dimensionless stress, σ', shown in a polar plot as a function of shell orientation. Flow is parallel to the ordinate of the graph, moving down from the top of the page. The length of a line from the graph's origin to the appropriate curve at a given angle is a measure of the dimensionless stress for a limpet with its anterior–posterior axis oriented in that direction. For example, if the animal is turned broadside to the flow (90 °), the dimensionless stress is approximately 0.2 when water velocity is 25 m s^{-1}. The broken curve shows the dimensionless stress for a cone with a height-to-length ratio similar to that of *Lottia gigantea*.

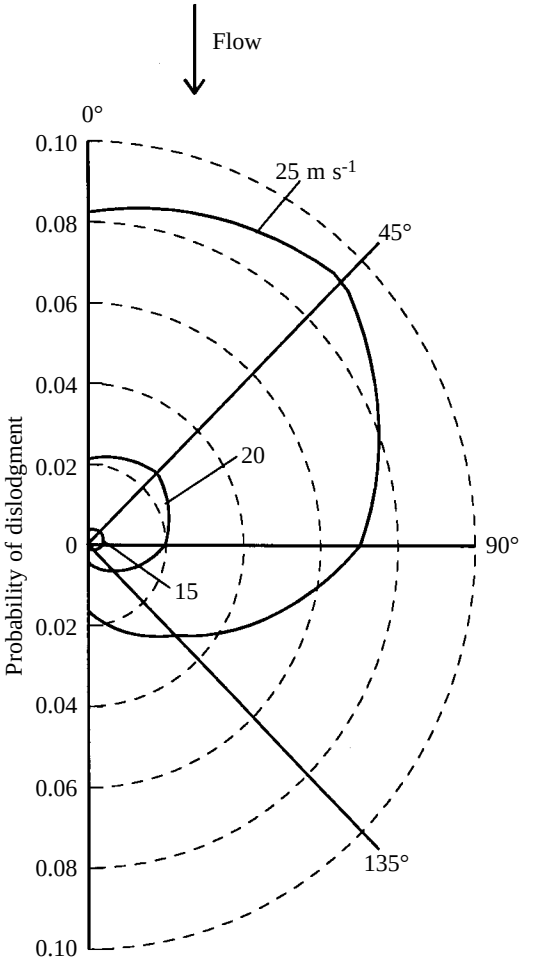

Fig. 11. The probability of dislodgment as a function of orientation to the flow and water velocity for a stationary limpet. This is a polar plot, as in Fig. 10. For example, if the animal is oriented with its anterior–posterior axis perpendicular (90 °) to a flow of 25 m s^{-1}, the risk of dislodgment is approximately 7 %. Dashed lines are lines of constant probability.

probability that a limpet will be dislodged by hydrodynamic forces. For all orientations and all water velocities below 25 m s^{-1}, the risk of dislodgment in shear is less than 0.2 %, and this miniscule risk will not be considered further.

Calculation of the risk of dislodgment in tension proceeds as follows. For an adult limpet of a representative length (5.00 cm), the proportional width is 3.74 cm and the planform area is 0.00147 m^2. From the relationships given in Table 1, we know that a limpet of this size can (on average) resist a tensile force of 190 N when stationary and 38 N when crawling rapidly. From equation 8, we can calculate the dynamic pressure, p_d, at any given velocity. At any given angle to the oncoming flow and for any given water velocity, the product of dynamic pressure and the maximal non-dimensional stress acting on the foot (Fig. 10) is the tensile force per planform area imposed on the limpet (the tensile stress). In turn, the product of this stress and A_{pl} gives the tensile force imposed. This tensile force divided by the predicted dislodgment force provides the normalized force, $F_{N,T}$, imposed by flow. Normalized force can then be inserted into the equation for the appropriate cumulative probability curve (Table 2) to estimate the likelihood that the limpet will be dislodged (Figs 11, 12). In these figures, risk is displayed as a polar plot (see Fig. 10). Again, 0 ° is taken to be towards the top of the page. If a line is extended from the origin in the direction of the shell's anterior–posterior axis, the length of that line when it crosses the curve for a given velocity is proportional to the risk at that particular orientation. For example, in Fig. 11, if the limpet's apex is 45 ° from an oncoming flow of 25 m s^{-1}, the risk of dislodgment is approximately 9 %.

The probability of dislodgment is quite low for stationary limpets regardless of their orientation (Fig. 11). At 20 m s^{-1} (an equivalent velocity in excess of the maximum recorded at all but one of our sites), the probability is less than 3 %. In contrast, at 20 m s^{-1}, more than 90 % of rapidly moving limpets would be dislodged unless they were oriented with their apex

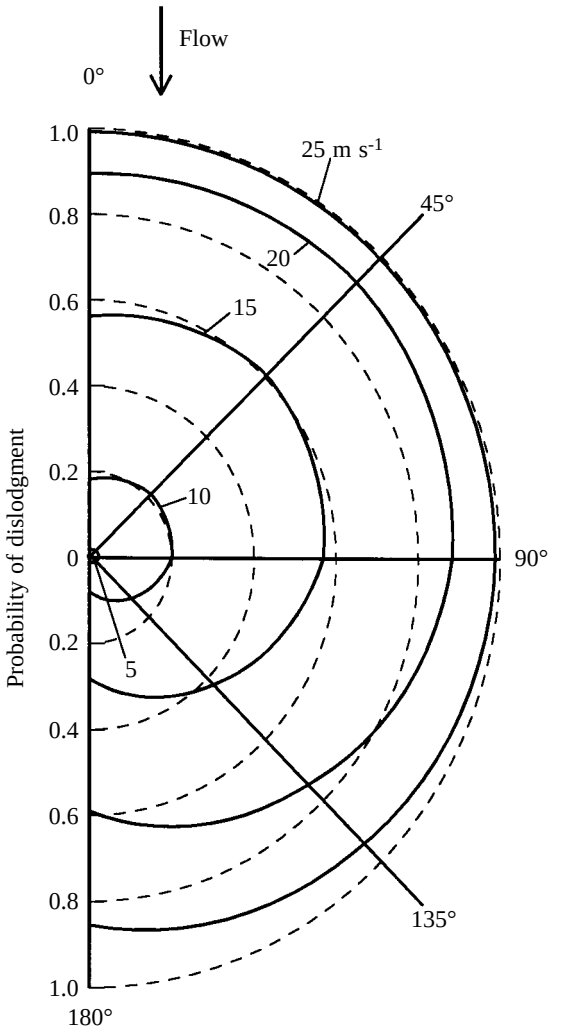

Fig. 12. The probability of dislodgment as a function of orientation to flow and water velocity for a moving limpet. Values are plotted as for Fig. 11.

downstream (Fig. 12). Even with the apex downstream, approximately 60 % would be dislodged.

These predictions of risk are based on calculations using measured drag and lift coefficients and an estimation of the maximal water velocity that limpets are likely to experience. We have ignored the effect noted by Gaylord (1997, 1999, 2000) in which the initial contact of a broken wave with an intertidal object produces a force that may be substantially larger than that predicted by theory. Is it possible that these 'impingement' forces may place limpets at substantial risk? We feel that the answer is 'no,' for two reasons. First, as reported below, our measurements of survivorship at one wave-exposed site suggest that limpets indeed survive quite well in the face of large breaking waves. Second, the velocities we have used in our calculations are themselves based on forces recorded in the field. If there is a large impingement effect, it is likely to act on our recording dynamometers, thereby resulting in an inflated estimate of the velocity. In other words, if the effect of impingement is the same on limpets as it is on our dynamometers, this factor has already been included in our calculations.

Note that our calculations of risk are potentially sensitive to variations in the lift coefficient, and the coefficients we use are based on extrapolations of C_L to velocities considerably higher than those used in our measurements. For example, the lift coefficients we have used for a velocity of $20\,m\,s^{-1}$ are on average 24 % lower than those actually measured at $5\,m\,s^{-1}$. The effect of any inaccuracy in our extrapolations is likely to be minor, however. For instance, if we were to assume that the lift coefficient did not decrease at all at high Reynolds number and use in our risk calculations the lift and drag coefficients made at the highest Reynolds numbers available in the laboratory, the predicted risk for a stationary limpet at a water velocity of $20\,m\,s^{-1}$ would still be quite low: 5.5 % as opposed to the 2.5 % calculated using the extrapolated values for C_L and C_D. The accuracy of our extrapolations for lift and drag coefficients can only be determined through empirical measurements at higher velocities than those currently available to us.

Orientation in the field

The distribution of orientations in the field is shown in Fig. 13. The largest fraction of limpets are indeed oriented head-down (270 °), but this trend was not statistically significant (Rayleigh r=0.053, P>0.50, N=172). In other words, in contrast to the data of Abbott (1956), the measurements conducted here cannot distinguish the orientation of limpets from a random orientation with respect to gravity or (if there is a preferred direction of wave-induced flow) with respect to flow.

Survivorship

Of the 65 limpets tagged in December 1997, 21 identifiable tagged individuals were present in June 1998 (filled circles,

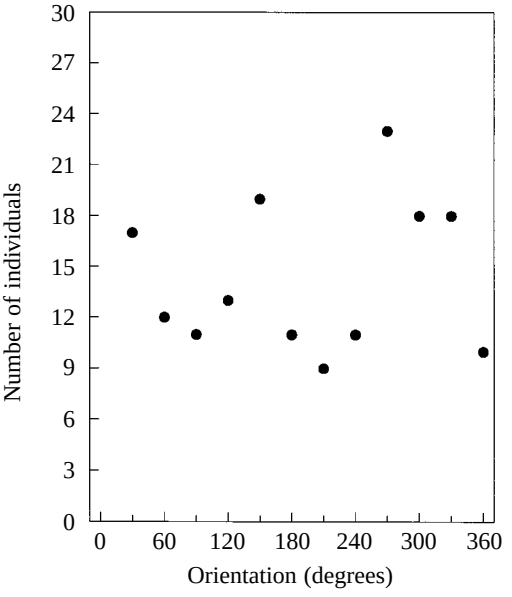

Fig. 13. The distribution of limpet orientations in the field.

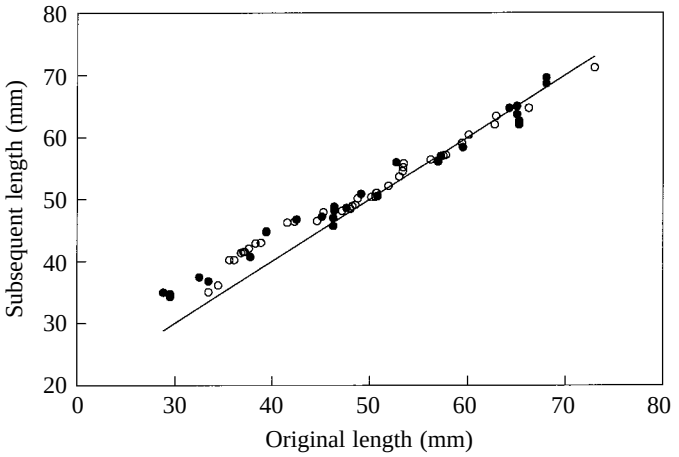

Fig. 14. Lengths of limpets at our field site in June 1998 plotted as a function of length in December 1997. The solid line is the line of equivalence. Filled circles denote individuals that retained their tags; open circles are for individuals assumed to have lost their tags.

Fig. 14). Note that several of these tagged limpets decreased in size, probably because of chipping of the shell (see Shanks and Wright, 1986). Forty-two other individuals with lengths greater than 28 mm were found on the rock face in June. Fifteen of these 42 limpets showed evidence of having been tagged (tag remnants or a residue of glue), but could not be positively identified. Three of the 42 showed no evidence of having been tagged, had lengths less than any tagged individuals and were probably local residents that had previously been too small to be tagged. These three limpets were excluded from further consideration. The lengths of the remaining 39 unidentified limpets are shown as open circles in Fig. 14. To create this figure, the lengths of the unidentified limpets were ranked in decreasing order and matched with a similarly ordered list of the initial lengths of the 39 largest original limpets for which a tag was not present in the June survey. The lengths of the 39 unidentified limpets correspond very well to the expected lengths of previously marked individuals, and (given the isolation of this rock face and the homing and territorial behavior of *L. gigantea*) we propose that these 39 individuals have simply lost their tags. Thus, at least 36 *L. gigantea* (21 with tags plus 15 with evidence of having been tagged) survived the winter storm season at this site, a survival rate of 54 %. If the 24 untagged individuals simply lost their tags, 60 of 65 individuals (92 %) survived. Even if a few of the unmarked limpets present in June were immigrants replacing dislodged individuals, it seems clear that survivorship among this population is quite high.

The data for the marked individuals (filled circles, Fig. 14) suggest that small limpets (28–45 mm length) grew 2–4 mm in the 7 months of this experiment, whereas large limpets (>45 mm length) grew an amount too small to measure or decreased in length. The slow growth among larger limpets suggests that these individuals may be many years old, providing additional evidence that the risk of dislodgment at this site is small.

Discussion

In general, the results of this study on actual limpet shells reinforce the conclusions drawn by Denny (2000) on the basis of conical models. The exceptional ability of *L. gigantea* to adhere to a rocky substratum allows the animal's shell to differ from a hydrodynamically optimal shape without incurring dire consequences for survival. The result is a shell that appears to have been 'good enough' in its interaction with flowing water, at the same time that it was being fine-tuned by other selective pressures to act as an effective bulldozer.

The ability to accommodate conflicting functional requirements highlights two aspects of the limpet's mechanics. First, Denny (2000) noted that, if the apex of a conical shell is displaced forward, the shell experiences an increased dimensionless risk when the apex is upstream. Although the anatomical apex of *L. gigantea* is far from the center of the shell, the topographical apex is near the center (Fig. 3), and at high water velocities the dimensionless stress is only slightly greater than that of a comparable right (symmetrical) cone (Fig. 10). In this respect, the overall shape of the shell has largely compensated for the deleterious effect of an anterior shift in the anatomical apex. This compensation has not adversely affected the hydrodynamic properties of the shell at other orientations. Indeed, when the animal's head is downstream, the dimensionless stress is substantially less than that found in a symmetrical cone, the same effect noted for models by Denny (2000). The rounded shape of the actual limpet shell thus incorporates the advantages of an apex-forward design (low risk when posterior into the flow) while accruing little of the disadvantages (a substantially increased risk when facing into the flow).

Second, the adhesive strength of *L. gigantea* is such that the shape of the shell has little effect on survivorship. For example, when the limpet is stationary and maximally adherent, the imposition of an extreme water velocity (25 $m\,s^{-1}$) is predicted to leave 90.7 % of limpets intact. The maximal dimensionless stress of a *L. gigantea* shell at 25 $m\,s^{-1}$ (0.217) is approximately 21 % larger than the minimal value (0.177) for a symmetrical cone with the optimal height-to-length ratio of 0.53 (Denny, 2000). Changing the shape of the shell of *L. gigantea* to reduce its dimensionless stress to the lowest measured for symmetrical cones would increase survivorship from 90.7 to 94.8 %. This small increase in survivorship is for an extreme water velocity; at lower water velocities, the increase in survivorship is even smaller. Thus, a drastic shift in shell shape (increasing the height-to-length ratio by a factor of almost 2.5, from 0.22 to 0.53) would result in only a 4.1 % increase in survivorship for those animals experiencing the maximal water velocity imposed by the environment.

In contrast, if a limpet is caught broadside by a large wave (an equivalent velocity of 25 $m\,s^{-1}$) in the midst of an escape response, only 0.5 % of animals would survive. If the dimensionless stress were reduced by 21 %, 2.4 % of escaping animals would survive. Relative to the extant limpet, the 'optimal' limpet would survive nearly five times better, an apparently large advantage. Note, however, that the increase in

absolute survivorship is only 1.9 %. Thus, if an individual limpet is reckless enough to be caught by a large wave in the midst of an escape, its chance of surviving is very small compared with that of its stationary neighbors regardless of its shape. In this case, the advantages of prudent locomotory behavior far outweigh the effects of shell shape.

In the absence of other selective factors, the small increases in survivorship that would accompany a shift to a more high-spired shell might act as an effective guide to the evolution of shell shape in *L. gigantea*. However, the relatively small magnitude of the effect of shell shape on hydrodynamic survivorship makes it easier to understand why, in the presence of counteracting selective factors (such as the advantages of an anterior 'plough'), selection by hydrodynamic forces has not resulted in a shell that is hydrodynamically optimal.

Note that we were unable to measure the adhesive strength of limpets during their normal foraging locomotion, and it seems likely that their adhesive abilities are greater while foraging than during the escape reactions used in our experiments. Thus, our prediction of the risk of dislodgment during locomotion is likely to overestimate the actual risk encountered from day to day. For example, Miller (1974) found that the adhesive tenacity of a variety of crawling gastropods was typically 33.4 % of their stationary tenacity. In contrast, for the size of *L. gigantea* assumed in our calculations here (length 5 cm), the tenacity during escape locomotion is only 20 % of the stationary tenacity. If we assume that the tenacity of *L. gigantea* during foraging is 33.4 % of its stationary tenacity (and that the shape of the cumulative probability curve is the same as for stationary animals), only 2.9 % of limpets would survive the imposition of a 25 $m\,s^{-1}$ water velocity. If the shell were optimally shaped, however, 16.2 % would survive. A 21 % reduction in dimensionless stress might therefore result in a 5.6-fold relative increase (a 13.3 % absolute increase) in survivorship among foraging individuals, a substantial and potentially important effect. The fact remains, however, that this effect would still be coupled to the loss of 83.8 % of limpets exposed to the extreme flow. Under these circumstances, *L. gigantea* may well decide to reduce its risk of dislodgment by choosing not to crawl, and Judge (1988) and Wright (1978) have shown that *L. gigantea* indeed reduces its feeding time when large hydrodynamic forces are applied. Given that our field data tentatively suggest that more than 90 % of *L. gigantea* survived the stormy season at an exposed site, the behavioral response to imposed force appears to be highly effective. In other words, the limpet's behavior is likely to ensure strong adhesion at times of maximal flow, thereby indirectly reducing the selective value of slight changes in shell shape.

In the past, questions regarding the evolved shape of limpet shells have focused on mechanical survivorship and physiology. For example, Vermeij (1993) and Lowell (1986, 1987) have suggested that the low-spired shape of limpet shells is an adaptation to avoiding crab predation, and D. R. Lindberg and W. F. Ponder (in preparation) suggest that it is in part an adaptation that increases the size of the pallial cavity, allowing for a larger gill and a consequent ability to withstand periods of low oxygen availability. Branch (1981) reviewed the evidence that shell shape has evolved to reduce the likelihood of desiccation stress. The prediction here that crawling limpets are highly susceptible to dislodgment while stationary limpets are virtually immune suggests that the course of evolution in shell shape may have had a substantial behavioral component. In effect, the animal has behavioral control over the trade-off between the risk of dislodgment and the time spent foraging and defending its territory. It appears, then, that the trade-off between the conflicting demands of hydrodynamic forces and aggressive behavior may best be examined in terms of foraging time (and thereby in terms of the rate of caloric intake and the consequent rates of growth and reproduction) rather than in terms of the risk of dislodgment.

List of symbols

a	acceleration
AA	anatomical apex
A_{pl}	planform area (=aperture area)
A_{pr}	profile area
b	coefficient (equation 6)
c	coefficient (equation 6)
C_D	drag coefficient
C_L	lift coefficient
C_M	inertia coefficient
d	coefficient (equation 6)
D	drag
$F_{N,S}$	normalized dislodgment force, shear
$F_{N,T}$	normalized dislodgment force, tension
F_P	predicted dislodgment force
$F_{P,S}$	predicted dislodgment force, shear
$F_{P,T}$	predicted dislodgment force, tension
F_S	dislodgment force, shear
F_T	dislodgment force, tension
H	shell height
i	rank
I	accelerational force
L	lift
n	number of samples
p_d	dynamic pressure
P	probability
Re	Reynolds number
T	tensile force
TA	topographic apex
u	water velocity
V	volume
W	shell width
y_{lc}	moment arm for lift
z_{dc}	moment arm for drag
α	regression coefficient (equation 2)
β	regression coefficient (equation 2)
λ	length of shell
ρ	water density
σ	tensile stress on basal adhesive

σ'	normalized tensile stress
τ	shear stress on basal adhesive
τ'	normalized shear stress

We thank B. Gaylord for his measurements of the inertia coefficients, K. Denny for assistance with field work and B. Hale, E. Nelson, J. Nelson and L. Hunt for their helpful comments. This study was funded by NSF grant OCE 9115688 to M.W.D.

References

Abbott, D. P. (1956). Water circulation in the mantle cavity of the owl limpet *Lottia gigantea* Gray. *Nautilus* **69**, 79–87.

Batchelor, G. K. (1967). *An Introduction to Fluid Dynamics.* Cambridge: Cambridge University Press.

Bell, E. C. and Denny, M. W. (1994). Quantifying 'wave exposure': a simple device for recording maximum velocity and results of its use at several field sites. *J. Exp. Mar. Biol. Ecol.* **181**, 9–29.

Branch, G. M. (1981). The biology of limpets: physical factors, energy flow and ecological interactions. *Oceanogr. Mar. Biol. Annu. Rev.* **19**, 235–380.

Cacceci, M. S. and Cacheris, W. P. (1984). Fitting curves to data: the simplex algorithm is the answer. *Byte* **May**, 340–362.

Denny, M. W. (1988). *Biology and the Mechanics of the Wave-Swept Environment.* Princeton: Princeton University Press.

Denny, M. W. (1989). A limpet shell that reduces drag: laboratory demonstration of a hydrodynamic mechanism and an exploration of its effectiveness in nature. *Can. J. Zool.* **67**, 2098–2106.

Denny, M. W. (1993). *Air and Water*. Princeton: Princeton University Press.

Denny, M. W. (1995). Predicting physical disturbance: mechanistic approaches to the study of survivorship on wave-swept shores. *Ecol. Monogr.* **65**, 371–418.

Denny, M. W. (2000). Limits to optimization: fluid dynamics and the evolution of shape in limpet shells. *J. Exp. Biol.* **203**, 2603–2622.

Denny, M. and Gaylord, B. (1996). Why the urchin lost its spines: hydrodynamic forces and survivorship in three echinoids. *J. Exp. Biol.* **199**, 717–729.

Fisher, W. K. (1904). The anatomy of *Lottia gigantea* Gray. *Zool. Jb. Anat.* **20**, 1–66.

Gaines, S. D. and Denny, M. W. (1993). The largest, smallest, highest, lowest, longest and shortest: extremes in ecology. *Ecology* **74**, 1677–1692.

Gaylord, B. (1997). Consequences of wave-induced water motion to nearshore macroalgae. PhD thesis, Stanford University, Stanford, California.

Gaylord, B. (1999). Detailing agents of physical disturbance: wave induced velocities and accelerations on a rocky shore. *J. Exp. Mar. Biol. Ecol.* **239**, 85–124.

Gaylord, B. (2000). Size, scaling and compliant design in intertidal organisms: implcations of fine-scale features of surf-zone flows. *Limnol. Oceanogr.* **45**, 174–188.

Gumbel, E. J. (1958). *Statistics of Extremes.* New York: Columbia University Press.

Judge, M. L. (1988). The effects of increased drag on *Lottia gigantea* (Sowerby 1834) foraging behaviour. *Funct. Ecol.* **2**, 363–369.

Lowell, R. B. (1986). Crab predation on limpets: predator behavior and defensive features of the shell morphology of the prey. *Biol. Bull.* **171**, 577–596.

Lowell, R. B. (1987). Safety factors of tropical *versus* temperate limpet shells: multiple selection pressures on a single structure. *Evolution* **41**, 638–650.

Miller, S. L. (1974). Adaptive design of locomotion and foot form in prosobranch gastropods. *J. Exp. Mar. Biol. Ecol.* **14**, 99–156.

Morris, R. H., Abbott, D. P. and Haderlie, E. C. (1980). *Intertidal Invertebrates of California.* Stanford: Stanford University Press.

Sarpkaya, T. and Isaacson, M. (1981). *Mechanics of Wave Forces on Offshore Structures*. New York: Van Nostrand-Reinhold.

Shanks, A. L. and Wright, W. G. (1986). Adding teeth to wave action: the destructive effects of wave-borne rocks on intertidal organisms. *Oecologia* **69**, 420–428.

Sprugel, D. G. (1983). Correcting for the bias in log transformed allometric equations. *Ecology* **64**, 209–210.

Stimson, J. (1970). Territorial behavior of the owl limpet, *Lottia gigantea*. *Ecology* **51**, 113–118.

Vermeij, G. J. (1993). *A Natural History of Shells.* Princeton: Princeton University Press.

Vogel, S. (1994). *Life in Moving Fluids.* Second edition. Princeton: Princeton University Press.

Wright, W. G. (1978). Aspects of the ecology and behavior of the owl limpet, *Lottia gigantea* Sowerby, 1834. *West. Soc. Malacol. Annu. Rep.* **11**, 7.

Zar, J. H. (1974). *Biostatistical Analysis.* Englewood Cliffs: Prentice-Hall.